Densification of UO2 pellets by microwave sintering using an instrumented multimode cavity

Clémence Petit, Christophe Meunier, François Valdivieso, Jérémy Croquesel, Sylvie Pillon, Anne-Charlotte Robisson, Julien Martinez, Florent Lemont

Densification of UO_2 pellets by microwave sintering using an instrumented multimode cavity

C. Petit[a*], C. Meunier[a], F. Valdivieso[a], J. Croquesel[a,b], S. Pillon[b], A.C. Robisson[b], J. Martinez[c], F. Lemont[c]

[a] Mines Saint-Etienne, Université Lyon, CNRS, UMR 5307 LGF, Centre SMS, F-42023 Saint-Etienne France

[b] CEA/DES/IRESNE/DEC/SETC, Centre de Cadarache, 13115 Saint-Paul-lez-Durance, France

[c] CEA/DES/ISEC/DMRC/STDC/LRVE, Centre de Marcoule, BP17171, 30207 Bagnols sur Cèze, France

* Corresponding author: Clémence Petit, clemence.petit@mines-stetienne.fr

Mines Saint-Etienne, Université Lyon, CNRS, UMR 5307 LGF, Centre SMS, F-42023 Saint-Etienne France, Phone : +33 4 77 42 02 23

Abstract

A study of microwave sintering of uranium dioxide pellets has been performed with the aim to densify the material. Microwave sintering heating has been carried out in a 2.45 GHz multimode cavity, designed to fit the different requirements linked to sintering of nuclear ceramics. Hybrid and direct microwave heating (*i.e.*, with and without susceptor) conditions were carried out. In the hybrid condition, thermal cycles at temperatures up to 1700°C, with a heating rate of 20°C/min and dwell times of 10-60 min could be applied to the samples. The sintered specimens exhibited high values of densities (92.6-94.6 % of theoretical density) with a grain size range of 9.1-11.8 µm, which is close to the results obtained with conventional sintering with longer thermal cycles. The pellet tested in the direct configuration only heated

until 950°C, showing the impossibility to heat UO_2 in a microwave furnace without the help of a susceptor.

Keywords: Uranium dioxide, Nuclear fuel, Microwave sintering, Densification

1. Introduction

Uranium dioxide (UO_2) has been widely used as nuclear fuel in light and heavy water reactors [1]. The pellets are generally fabricated by the conventional processes for ceramic materials. The oxide powder is first mixed with organic additives and then compacted into pellets. The green pellets are subsequently sintered in the temperature range 1600-1800°C, in a reducing atmosphere with a dwell time of 3 to 10 hours [2-4]. These sintering parameters are necessary to achieve high final density (more than 95 % TD, Theoretical Density). However, this leads to long duration of thermal cycle and thus, high consumption of electrical energy and time. Consequently, there is a need to reduce the environmental impact of sintering in the ceramic processes.

In the last decades, microwave sintering appeared as an interesting alternative to conventional heating. Different studies showed the possibility of densifying ceramics with lower heating rate and shorter dwell time [5-8]. Contrary to the resistive furnaces, in microwave heating, the ceramics are directly heated by absorption of microwaves, leading to fast and volumetric heating [9,10]. Few authors tried to sinter by microwave UO_2 pellets. Subramanian *et al.* reached high density of 95.5 % TD but they did not give any indication about temperature measurement [11]. Yang *et al.* also obtained dense pellets with low heating rates of 5-7°C/min. But, the samples sintered at 20-30°C/min exhibited cracks [12]. Despite first interesting results, these authors did not provide detailed information about the sintering parameters (*e.g.*, temperature measurement). This problem mainly comes from the absence of

adapted measurement techniques for microwave sintering, especially for temperature measurement.

In a recent paper, Croquesel *et al.* presented an instrumented multimode microwave cavity specifically designed to study sintering of nuclear ceramics [13]. This cavity has been optimized to heat samples until high temperature (1600-1700°C range) under reducing atmosphere with high heating rates. Different devices have been included to monitor sintering: optical dilatometry to follow the pellet shrinkage during sintering and pyrometers to measure precisely the temperature.

The aim of this paper is to present the study performed in this cavity with UO_2 pellets. A sintering study has been carried out with varying parameters (temperature, dwell time). The sintered samples have been characterized in terms of final density and grain size. These data are also compared with the ones obtained for pellets sintered in conventional sintering. A discussion about the interaction between the material and the microwaves is also proposed.

2. Materials and methods

2.1. Sample preparation

Uranium dioxide powder obtained by the conventional ADU (ammonium diuranate) conversion process (*supplier TU2, lot TU2-91*) was used as the starting material in this study. The O/U ratio was 2.05 and the specific surface area was 3.02 m^2/g. The powder was uniaxially pressed as cylinders of 10-mm diameter and 11-mm height. The green bodies had a density of around 5.85 g/cm^3 (53 % of theoretical density, taking into account a density of 10.97 g/cm^3 for fully dense UO_2 pellet).

2.2. Heating treatments in the microwave cavity

Microwave sintering (MS) was carried out in the multimode cavity working at 2.45 GHz described in [13]. This reference presents how the cavity was designed and how it works. The sample was placed inside the sintering cell described in [13]. This cell is made of porous aluminosilicate plates used as insulators. Two zirconia plates (3Y-TZP) were used as susceptors (to help heating). A series of sintering tests was made with the susceptors inside the sintering cell (hybrid configuration) in order to find the best sintering parameters to densify the samples. The following thermal cycle was applied: heating at a rate of 4°C/min until 150°C (to avoid sample cracking) and then heating at a rate of 20°C/min until the peak temperature (1650 or 1700°C) with different dwell times (10 - 30 - 60 min). The sintering atmosphere is a mixture of argon and 4% hydrogen. The microwave generator was switched off just at the end of the dwell time, enabling a natural cooling of the samples. The temperature was measured by pyrometers which were previously calibrated [14]. During the heating cycle, the measured temperature and powers (incident, absorbed and reflected powers) were recorded thanks to a Labview interface [13].

To complete this study, a UO_2 pellet was also heated with the same microwave cavity but without the use of the susceptor in the sintering cell (direct configuration). In this case, the following heating program was applied: heating at 4°C/min from room temperature until 150°C, then heating at 20°C/min until the maximum temperature achievable. The aim was to determine the highest temperature attainable without susceptor and to understand better the microwave/material interactions. Table 1 lists the different samples tested in this study with the parameters used for the heating cycles.

2.3. Characterization of the sintered samples

The density of the sintered samples was measured thanks to Archimedes' method with absolute ethanol. The diametral shrinkage was recorded thanks to the optical dilatometry

device. The detailed procedure can be found in Ref [15,16]. The diametral shrinkage is measured for MS whereas shrinkage along the height is measured for CS (conventional dilatometric analysis). Therefore, in order to compare the shrinkages in MS and CS, it is necessary to calculate the anisotropy shrinkage coefficient α, assumed to be constant during the whole sintering process:

$$\alpha = \frac{\phi_f - \phi_0}{\phi_0} . \frac{h_0}{h_f - h_0} \quad (1)$$

Where h_0 and h_f represent respectively the initial and final sample height, ϕ_0 and ϕ_f represent respectively the initial and final diameter.

The microstructures were observed using Scanning Electronic Microscopy (SEM, *Zeiss SUPRA55VP, Carl Zeiss Microscopy GmbH, Oberkochen, Germany*). Before observation, the samples were cut to characterize the bulk microstructure thanks to a high precision wire saw (*WS-22*). They were then embedded in a methacrylate resin (*LamPlan 605*) and polished down to 1 µm diamond suspension. To reveal the grain boundaries, a final polishing step with colloidal silica (*MasterMet 2, Buehler*) was added. The images were obtained with an accelerating voltage of 20 kV with a backscattered electron detector to detect the grain boundaries. UO_2 being an insulator at room temperature, a low vacuum configuration (30 Pa of dinitrogen) was used to avoid gold-coating the samples. The average grain sizes were determined thanks to the linear intercept method described by Mendelson [17] applied on 250 grains for each sample. A statistical correction factor of 1.56 was applied to calculate the average grain size.

Five SEM images per sintered samples were also used for determination of an estimate of final relative density. The images were processed with Image J software [18] with the following steps: improvement of the quality of the images by adjustment of contrast and brightness, application of a median filtering over one pixel and thresholding to separate the grains and the pores. The final relative density was determined as the ratio of the number of

pixels belonging to the pores over the total number of pixels in the image. The values were used as comparison purposes with the values obtained by Archimedes method.

3. Results and discussion

3.1. Characterization of the sintered samples in the hybrid configuration

Table 2 presents the final densities and the average grain sizes of the sintered pellets. Density increased with increasing sintering temperatures and holding times as generally observed for ceramic materials. The highest value of density reached in MS was 10.37 g/cm^3 (94.6 %TD). In previous studies, values in the range 92-93.9 %TD were found for UO_2 pellets sintered in conventional furnace with the following conditions: UO_2 powder synthesized by ADU process, sintering cycle 1600°C / 4 h / 1°C/min, Ar / 4% H_2 atmosphere [3,4]. Therefore, the MS samples were densified with a shorter holding time (max. 1 h) and a higher heating rate (20°C/min). As previously said, Yang *et al.* [12] attempted to sinter specimens at 20 and 30°C/min but the samples exhibited cracks. They reached highest densities (> 96 % TD) but at lower heating rate (5-7°C/min). To the best of our knowledge, it is the first time that UO_2 pellets were densified without cracks with a thermal cycle combining such high heating rate and short holding duration.

The radial shrinkage and the shrinkage rate versus temperature are plotted in Figure 1a for the sample P1700-10. For comparison purpose, dilatometric data for a CS sample obtained from a previous study [3] are also shown in Figure 1b. This latter sample was obtained in the following conditions: UO_2 powder synthesized with the ADU process, sintering cycle 1600°C / 1°C/min / 4 hours, under Ar/5%H_2. The final radial shrinkage for the P1700-10 sample was -

19% whereas the linear shrinkage for CS sample was -16%. This small difference can be related to the anisotropic shrinkage coefficient, which is slightly higher than 1 (1.13 calculated for the P1700-10 pellet). For the P1700-10 sample, the onset shrinkage temperature was around 950°C and the maximum shrinkage rate temperature was around 1260°C. These particular temperatures are higher for the CS sample: around 1050°C and 1350°C respectively (see Figure 1b). The lowering of these temperatures for MS with respect with CS has already been observed by other authors [19,20] for alumina samples. This observation could be viewed as an enhancement of densification under microwave, especially during the initial and intermediate stages. The authors proposed that a possible change of diffusion mechanism occurred during initial and intermediate sintering stages between CS and MS [20].

Figure 2 presents a SEM image of the P1700-10 polished surface. The microstructure is characterized by equiaxed grains with an average grain size in the range 9.1 – 11.8 µm (see Table 2). This range is in agreement with other values of grain sizes obtained in the literature for UO_2 samples in CS [21-24]. A slight increase of the grain size was obtained with increase of the dwell time for a given temperature, as expected. Table 2 also indicates the values of percentage of densification estimated by image analysis of the SEM images. These values are slightly different from the ones obtained by Archimedes method. This difference can be related to two problems linked to the image analysis. Firstly, image analysis is a surface analysis, leading to a loss of information compared to a 3D characterization. Then, a slight deterioration of some grains may have occurred during the polishing process, leading to an underestimation of the final relative density by image analysis.

Figure 3 presents different SEM images of P1700-10 sample taken at different locations along a line (from edge to center) in a cut plane. No microstructural difference are visible between the different images. In particular, no abnormal grain growth was noticed in some areas.

Therefore, the thermal gradients were low in the samples, indicating a homogeneous heating during microwave thermal cycle.

3.2. Microwave / material interaction

During microwave heating, materials couple with the electric field, absorb its energy in its bulk and dissipates it into heat [25]. Therefore, the specimens heat thanks to their own dielectric properties, especially the dielectric loss factor (ratio of the imaginary over the real part of dielectric complex permittivity). The dielectric properties vary with frequency and temperature and data is rarely found in the literature. In most oxide ceramics, the dielectric loss factor is low at room temperature and increase with temperature. It means that, at the beginning of the heating cycle, heating is often difficult and a susceptor (*i.e.*, a material having a high dielectric loss factor especially at room temperature) is needed to initiate heating [26].

In our previous paper [13], we showed the possibility to heat UO_2 pellets until 1700°C without electric arcs or plasma formation with zirconia susceptors. The sintering tests presented in this article confirm this assumption. Figure 4a, 4b, 4c and 4d present the temperature and powers vs time for the following pellets sintered with the susceptor: P1650-10, P1650-30, P1650-60 and P1700-10. The curves show that the set heating step was quite correctly followed thanks to PID regulation. A small instability around 800-900°C range visible in the four curves corresponds to the change of pyrometers used to measure the temperature. The holding time at maximum temperature was a little more difficult to maintain. Oscillations of +/- 10°C around the peak temperature are visible (see especially Figure 4a). In all the cases, the reflected power is lower than the absorbed power. It means that the susceptors allowed to concentrate the electric field between them (*i.e.*, where the UO_2 pellet was placed). The incident power was mainly concentrated between the two 3Y-TZP

plates, which then heated the pellet by radiation. That is why this type of microwave heating is called hybrid, that is to say: the pellets heat in the bulk thanks to direct coupling with microwave and on the surface by radiation of the susceptors. In spite of the good PID regulation, two small disturbance zones are visible in the heating step. Figure 4e and Figure 4f show focuses on the 200-700°C and 1200-1700°C ranges for the case of the P1650-30 pellet. The variation of the incident power is also represented. These two curves show low oscillations in the temperature increase in the 300-600°C and 1300-1600°C ranges. These low variations in temperature are accompanied by larger oscillations in incident power delivered by the PID regulation. The same observations can be done for the other samples (see Figure 4a, 4b and 4d). It is possible to relate these observations to the dielectric and electrical properties of UO_2 and 3Y-TZP. The event in the 300-600°C can be related to the evolution of dielectric properties of 3Y-TZP with temperature. Batt *et al.* measured real and imaginary parts of dielectric permittivity of 3Y-TZP from room to 1200°C [27]. The real part stays almost constant in the whole range while the imaginary part increases continuously, with a sharply increase between 400 and 500°C (value from 1 at 400°C to 10 at 500°C). Therefore, a sudden increase of the dielectric loss factor occurs in this temperature range. It can explain the difficulty to control heating rate in this temperature range and the disturbance observed in Figure 4e. Then, the increase of temperature was also difficult from 1300 to 1600°C. It can be related to the dielectric and electrical properties of UO_2. Very few studies exist about dielectric properties of UO_2. Gesi *et al.* [28] showed that the real part of the permittivity was constant (21) and the imaginary part increased from room temperature to 100°C (from 10^{-3} to 10^{-2}), at a frequency of 9.4 GHz. This study tends to prove that the dielectric loss factor of UO_2 increases with temperature. Electrical conductivity is also an important parameter for the microwave heating. Indeed, penetration depth of microwave is inversely proportional to electrical conductivity [25]. Bates *et al.* measured electrical conductivity for UO_2 samples

from room temperature to 2700°C [29]. An electrical conductivity of around 10^{-3} $\Omega^{-1}.cm^{-1}$ was found at room temperature and then increased with temperature. A sharper rise was observed from 1200°C. As an example, it increased from 0.42 $\Omega^{-1}.cm^{-1}$ at 1200°C to 4 $\Omega^{-1}.cm^{-1}$ at 1700°C. This increase of electrical conductivity can explain the difficulty to heat UO_2 in the 1300-1600°C range. But, the presence of 3Y-TZP allowed heating to continue. From 1000°C, the imaginary part of 3Y-TZP is higher than the real part. Therefore, the high dielectric loss factor of 3Y-TZP in this temperature range permitted to counterbalance the negative effect of the UO_2 properties.

Figure 5 presents the evolution of temperature and incident, absorbed and reflected powers with time for the P-Direct pellet. These curves enable to analyse the direct interaction between UO_2 and microwave, because of the absence of the ZrO_2 susceptors. From 150 to 400°C, a linear heating step is visible. Incident powers between 400 and 1000 W were needed to promote the sample heating. At higher temperature, the increase of temperature was more irregular and higher values of incident power were needed to continue heating. At 900°C, a sudden decrease of temperature occurred but was overcome by an increase of incident power up to more than 2000 W. It allowed for a second increase of temperature until 950°C. At this temperature, electric arcs appeared in the cavity, which led to the microwave switching off. The difficulty to heat the UO_2 pellet in the 400-950°C can be attributed to the increase of the electrical conductivity of UO_2 in this temperature range [29]. Contrary to the hybrid configuration, no susceptor was present to counterbalance this effect. Only the increase of incident power allowed heating to continue. But, at 950°C, the high value of incident power (2200 W) and the high electrical conductivity of UO_2 led to the formation of hot spots and, so of electric arcs. This temperature is too low to perform sintering of UO_2 in a direct microwave configuration. That is why a ZrO_2 susceptor was necessary to carry out sintering of UO_2 pellets at the required temperature (around 1650-1700°C).

4. Conclusion

This paper presented a sintering study of UO_2 pellets carried out in a dedicated and adapted microwave multimode cavity. The microwave device included a precise control of the heating cycle and a monitoring of shrinkage. Two configurations of heating were tested in the cavity: with and without the use of ZrO_2 susceptor to help heating of UO_2 (hybrid and direct configuration respectively). In the hybrid configuration, dense and crack-free UO_2 pellets were obtained. Relative densities in the 92 -95 % range and average grain size of around 10 µm were reached with shorter heating cycles compared to conventional sintering. In particular, a higher heating rate (20°C/min) and shorter soaking times (30-60 min) were used. The temperature vs time curves for MS with and without susceptors showed the influence of the electrical and dielectric properties of UO_2 and ZrO_2 on its coupling with microwaves. It was shown that a direct microwave heating of UO_2 was possible until 950°C. This confirmed the need to use a susceptor to heat it until the temperature range required for sintering. But, this also opens the way to a possible application of microwave heating to recycling of UO_2 pellets (which requires lower temperature).

5. Conflict of interest

None

6. Acknowledgements

The authors want to acknowledge Marilyne Mondon for its help for the SEM observations.

7. References

[1] M. Ho, E. Obbard, P.A. Burr, G. Yeoh, A review on the development of nuclear power reactors, Energy Procedia. 160 (2019) 459–466. https://doi.org/10.1016/j.egypro.2019.02.193.

[2] T.R.G. Kutty, P.V. Hegde, K.B. Khan, U. Basak, S.N. Pillai, A.K. Sengupta, G.C. Jain, S. Majumdar, H.S. Kamath, D.S.C. Purushotham, Densification behaviour of UO_2 in six different atmospheres, J. Nucl. Mater. 305 (2002) 159–168. https://doi.org/10.1016/S0022-3115(02)00934-0.

[3] S. Berzati, S. Vaudez, R.C. Belin, J. Léchelle, Y. Marc, J.-C. Richaud, J.-M. Heintz, Controlling the oxygen potential to improve the densification and the solid solution formation of uranium–plutonium mixed oxides, J. Nucl. Mater. 447 (2014) 115–124. https://doi.org/10.1016/j.jnucmat.2013.12.014.

[4] S. Vaudez, C. Marlot, J. Lechelle, Influence of chemical composition variations on densification during the sintering of MOX materials, Metall. Mater. Trans. E. 3 (2016) 107–111. https://doi.org/10.1007/s40553-016-0074-0.

[5] K.H. Brosnan, G.L. Messing, D.K. Agrawal, Microwave Sintering of Alumina at 2.45 GHz, J. Am. Ceram. Soc. 86 (2003) 1307–1312. https://doi.org/10.1111/j.1151-2916.2003.tb03467.x.

[6] I.N. Sudiana, R. Ito, S. Inagaki, K. Kuwayama, K. Sako, S. Mitsudo, Densification of Alumina Ceramics Sintered by Using Submillimeter Wave Gyrotron, J. Infrared Millim. Terahertz Waves. 34 (2013) 627–638. https://doi.org/10.1007/s10762-013-0011-6.

[7] C.J. Reidy, T.J. Fleming, S. Hampshire, M.R. Towler, Comparison of Microwave and Conventionally Sintered Yttria-Doped Zirconia Ceramics, Int. J. Appl. Ceram. Technol. 8 (2011) 1475–1485. https://doi.org/10.1111/j.1744-7402.2011.02608.x.

[8] A. Chanda, S. Dasgupta, S. Bose, A. Bandyopadhyay, Microwave sintering of calcium phosphate ceramics, Mater. Sci. Eng. C. 29 (2009) 1144–1149. https://doi.org/10.1016/j.msec.2008.09.008.

[9] K.I. Rybakov, E.A. Olevsky, E.V. Krikun, Microwave Sintering: Fundamentals and Modeling, J. Am. Ceram. Soc. 96 (2013) 1003–1020. https://doi.org/10.1111/jace.12278.

[10] M. Oghbaei, O. Mirzaee, Microwave versus conventional sintering: A review of fundamentals, advantages and applications, J. Alloys Compd. 494 (2010) 175–189. https://doi.org/10.1016/j.jallcom.2010.01.068.

[11] T. Subramanian, P. Venkatesh, K. Nagarajan, P.R. Vasudeva Rao, A novel method of sintering UO_2 pellets by microwave heating, Mater. Lett. 46 (2000) 120–124. https://doi.org/10.1016/S0167-577X(00)00153-1.

[12] J.H. Yang, K.W. Song, Y.W. Lee, J.H. Kim, K.W. Kang, K.S. Kim, Y.H. Jung, Microwave process for sintering of uranium dioxide, J. Nucl. Mater. 325 (2004) 210–216. https://doi.org/10.1016/j.jnucmat.2003.12.003.

[13] J. Croquesel, C. Meunier, C. Petit, F. Valdivieso, S. Pillon, A.C. Robisson, J. Martinez, F. Lemont, Design of an instrumented microwave multimode cavity for sintering of nuclear ceramics, Mater. Des. (2021) 109638. https://doi.org/10.1016/j.matdes.2021.109638.

[14] R. Macaigne, S. Marinel, D. Goeuriot, C. Meunier, S. Saunier, G. Riquet, Microwave sintering of pure and TiO_2 doped $MgAl_2O_4$ ceramic using calibrated, contactless in-situ dilatometry, Ceram. Int. 42 (2016) 16997–17003. https://doi.org/10.1016/j.ceramint.2016.07.206.

[15] D. Żymełka, S. Saunier, J. Molimard, D. Goeuriot, Contactless monitoring of shrinkage and temperature distribution during hybrid microwave sintering, Adv. Eng. Mater. 13 (2011) 901–905. https://doi.org/10.1002/adem.201000354.

[16] J. Croquesel, D. Bouvard, J.-M. Chaix, C.P. Carry, S. Saunier, Development of an instrumented and automated single mode cavity for ceramic microwave sintering: Application to an alpha pure alumina powder, Mater. Des. 88 (2015) 98–105. https://doi.org/10.1016/j.matdes.2015.08.122.

[17] M.I. Mendelson, Average grain size in polycrystalline ceramics, J. Am. Ceram. Soc. 52 (1969) 443–446. https://doi.org/10.1111/j.1151-2916.1969.tb11975.x.

[18] NIH National Institute of Health, Image J [in line]. Available on: http://imagej.nih.gov/ij/.

[19] D. Żymełka, S. Saunier, D. Goeuriot, J. Molimard, Densification and thermal gradient evolution of alumina during microwave sintering at 2.45GHz, Ceram. Int. 39 (2013) 3269–3277. https://doi.org/10.1016/j.ceramint.2012.10.015.

[20] F. Zuo, S. Saunier, C. Meunier, D. Goeuriot, Non-thermal effect on densification kinetics during microwave sintering of α-alumina, Scr. Mater. 69 (2013) 331–333. https://doi.org/10.1016/j.scriptamat.2013.05.016.

[21] X. Iltis, M. Ben Saada, H. Mansour, N. Gey, A. Hazotte, N. Maloufi, A new characterization approach for studying relationships between microstructure and creep damage mechanisms of uranium dioxide, J. Nucl. Mater. 474 (2016) 1-7 http://dx.doi.org/10.1016/j.jnucmat.2016.02.027

[22] Y. Harada, UO_2 sintering in controlled oxygen atmospheres of three-stage process, J. Nucl. Mater. 245 (1997) 217–223. https://doi.org/10.1016/S0022-3115(96)00755-6.

[23] Y.W. Lee, M.S. Yang, Characterization of HWR fuel pellets fabricated using UO_2 powders from different conversion processes, J. Nucl. Mater. 178 (1991) 217–226. https://doi.org/10.1016/0022-3115(91)90389-O.

[24] K.W. Song, K. Sik Kim, K. Won Kang, Y. Ho Jung, Grain size control of UO_2 pellets by adding heat-treated U_3O_8 particles to UO_2 powder, J. Nucl. Mater. 317 (2003) 204–211. https://doi.org/10.1016/S0022-3115(03)00080-1.

[25] R.R. Mishra, A.K. Sharma, Microwave–material interaction phenomena: Heating mechanisms, challenges and opportunities in material processing, Compos. Part Appl. Sci. Manuf. 81 (2016) 78–97. https://doi.org/10.1016/j.compositesa.2015.10.035.

[26] M. Bhattacharya, T. Basak, A review on the susceptor assisted microwave processing of materials, Energy 97 (2016) 306-338 http://dx.doi.org/10.1016/j.energy.2015.11.034306e338

[27] J. Batt, W.H. Sutton, J.G.P. Binner, T.E. Cross, A parallel measurement programme in high temperature dielectric property measurement: An update, (1995). https://www.osti.gov/biblio/269926 (accessed September 2, 2019).

[28] K. Gesi, J. Tateno, Dielectric constant of UO_2 at 9.4 GHz, Jpn. J. Appl. Phys. 8 (1969) 1358. https://doi.org/10.1143/JJAP.8.1358.

[29] J.L. Bates, C.A. Hinman, T. Kawada, Electrical conductivity of uranium dioxide, J. Am. Ceram. Soc. 50 (1967) 652–656. https://doi.org/10.1111/j.1151-2916.1967.tb15021.x.

Tables' and figures' captions

Table 1: List of the heated samples with the conditions of the heat treatment: hybrid (*i.e.*, with the use of susceptors) or direct (*i.e.*, without the use of susceptors) type of microwave heating, maximum temperature achieved and holding time

Table 2: Final density (by Archimedes method), percentage of densification estimated by image analysis and average grain size for the sintered pellets in hybrid configuration

Figure 1: Dilatometric data (a) for the P1700-10 sample and (b) for a UO_2 sample sintered in CS under Ar/5% H_2 (from [3])

Figure 2: (a) SEM image (back-scattered mode) of the P1700-10 sample and (b) corresponding binarized image for image analysis

Figure 3: SEM images of the P1700-10 sample taken at different locations in the cut plane: (a) scheme showing the location of the images and (b, c and d) the corresponding images

Figure 4: Temperature and incident, absorbed and reflected microwave powers vs time for the following pellets: (a) P1650-10, (b) P1650-30, (c) P1650-60 and (d) P1700-10. The panels (e) and (f) show magnified views of some parts of the graph shown in (c) in two temperature ranges: 200-700°C and 1200-1700°C

Figure 5: Temperature and incident, absorbed and reflected powers vs time for the pellet P-Direct

Table 1:

Name of the samples	Type of microwave heating	Maximum temperature (°C)	Holding time (min)
P1650-10	Hybrid	1650	10
P1650-30	Hybrid	1650	30
P1650-60	Hybrid	1650	60
P1700-10	Hybrid	1700	10
P1700-30	Hybrid	1700	30
P-Direct	Direct	950	-

Table 2:

Sample name	Density and % of densification (% TD) by Archimedes method	Estimated % of densification (%TD) by image analysis	Average grain size (µm)
P1650-10	10.15 (92.6)	88.9 ± 2.2	9.7 ± 3.4
P1650-30	10.19 (93.0)	91.7 ± 1.2	10.1 ± 3.3
P1650-60	10.37 (94.6)	90.4 ± 2.3	11.8 ± 3.9
P1700-10	10.16 (92.6)	92.1 ± 1.1	9.1 ± 2.5
P1700-30	10.37 (94.6)	88.2 ± 1.2	9.6 ± 3

Figure 1:

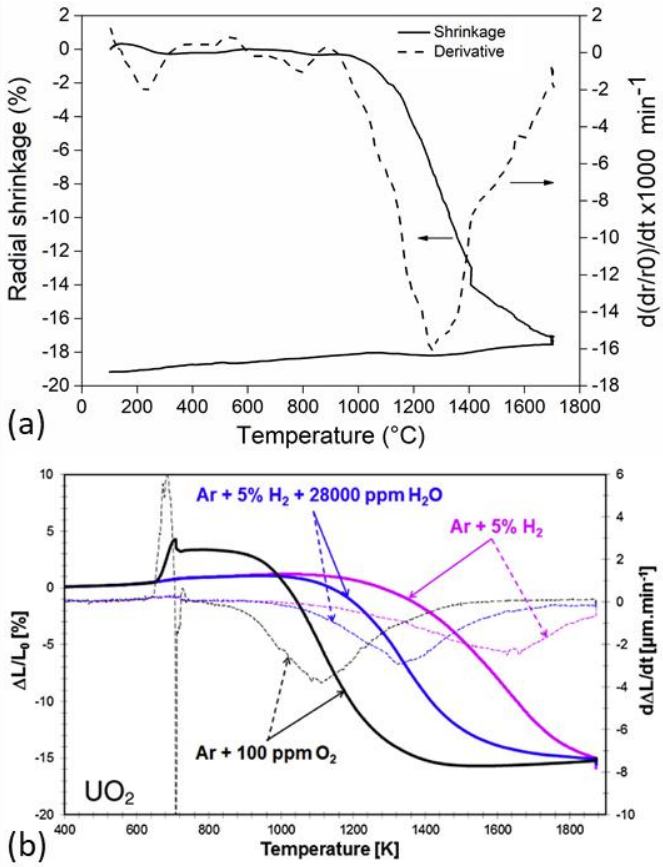
Shrinkage
Derivative
Radial shrinkage (%)
d(dr/r0)/dt x1000 min-1
Temperature (°C)
(a)
Ar + 5% H2 + 28000 ppm H2O
Ar + 5% H2
Ar + 100 ppm O2
UO2
ΔL/L0 [%]
dΔL/dt [µm.min-1]
Temperature [K]
(b)

Figure 2:

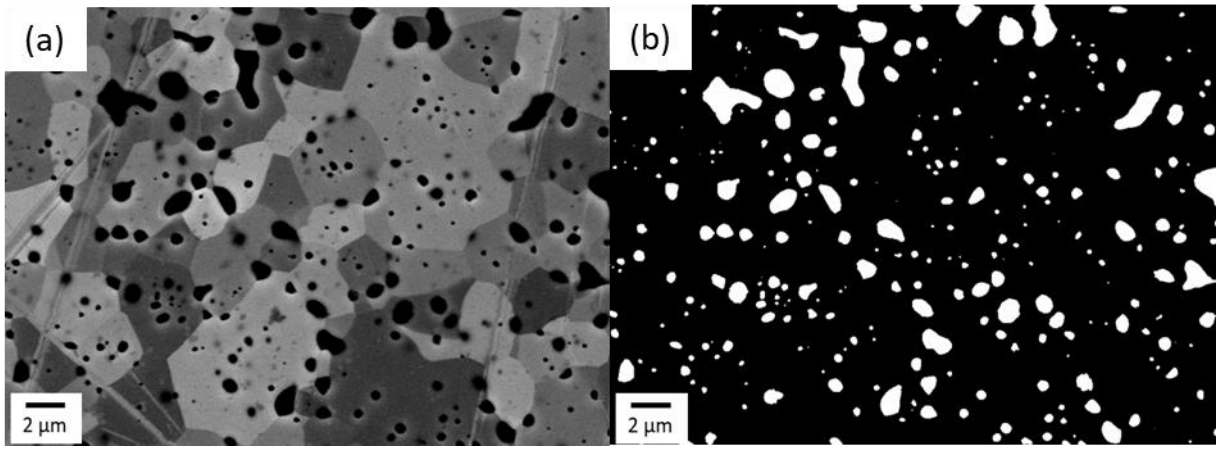

Figure 3:

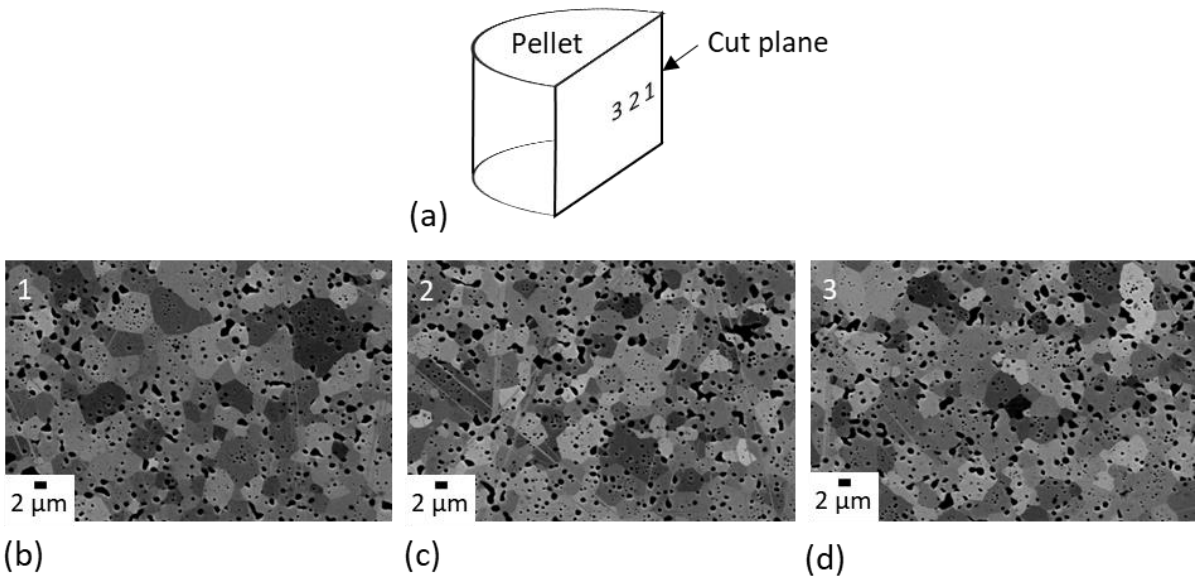

Figure 4:

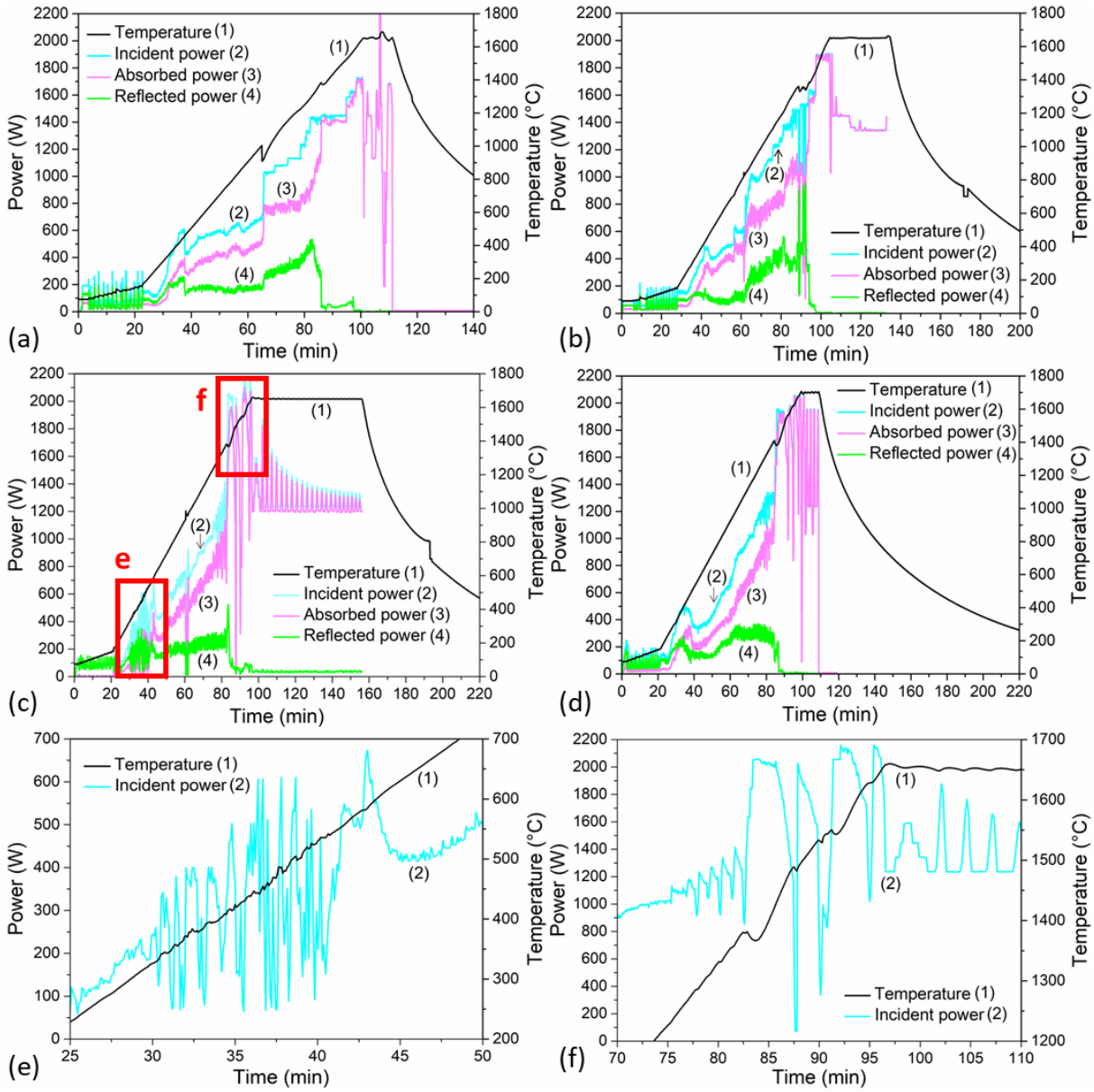
(a)
Temperature (1)
Incident power (2)
Absorbed power (3)
Reflected power (4)
Power (W)
Temperature (°C)
Time (min)
(b)
(c)
e
f
(d)
(e)
(f)

Figure 5:

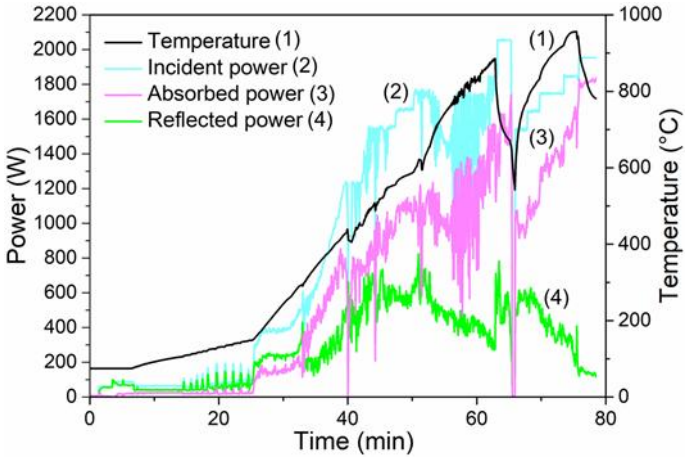
Temperature (1)
Incident power (2)
Absorbed power (3)
Reflected power (4)
(1)
(2)
(3)
(4)
Power (W)
Temperature (°C)
Time (min)
0
200
400
600
800
1000
1200
1400
1600
1800
2000
2200
0
20
40
60
80